HHS Public Access

Author manuscript

Acta Biomater. Author manuscript; available in PMC 2024 April 15.

Published in final edited form as:

Acta Biomater. 2023 April 15; 161: 285–297. doi:10.1016/j.actbio.2023.03.007.

Immune Cell Response to Orthopedic and Craniofacial Biomaterials Depends on Biomaterial Composition

Derek Avery[1], **Lais Morandini**[1], **Natalie Celt**[1], **Leah Bergey**[1], **Jamelle Simmons**[1], **Rebecca K. Martin**[2], **Henry J. Donahue**[1], **Rene Olivares-Navarrete**[1]

[1]Department of Biomedical Engineering, College of Engineering, Virginia Commonwealth University, Richmond, VA, United States

[2]Department of Microbiology and Immunology, School of Medicine, Virginia Commonwealth University, Richmond, VA, United States

Abstract

Materials for craniofacial and orthopedic implants are commonly selected based on mechanical properties and corrosion resistance. The biocompatibility of these materials is typically assessed *in vitro* using cell lines, but little is known about the response of immune cells to these materials. This study aimed to evaluate the inflammatory and immune cell response to four common orthopedic materials [pure titanium (Ti), titanium alloy (TiAlV), 316L stainless steel (SS), polyetheretherketone (PEEK)]. Following implantation into mice, we found high recruitment of neutrophils, pro-inflammatory macrophages, and $CD4^+$ T cells in response to PEEK and SS implants. Neutrophils produced higher levels of neutrophil elastase, myeloperoxidase, and neutrophil extracellular traps *in vitro* in response to PEEK and SS than neutrophils on Ti or TiAlV. Macrophages co-cultured on PEEK, SS, and TiAlV increased polarization of T cells towards Th1/Th17 subsets and decreased Th2/Treg polarization compared to Ti substrates. Although SS and PEEK are considered biocompatible materials, both induce a more robust inflammatory response than Ti or Ti alloy with high infiltration of neutrophils and T cells, which may cause fibrous encapsulation of these materials.

Keywords

Titanium; Titanium alloy; PEEK; 316L stainless steel; neutrophils; macrophages; T cells

1. Introduction

Craniofacial and orthopedic implants are some of the most successful clinical devices with well-documented patient outcomes that achieve a higher than 90% survival rate at >10 years [1]. The demand for these implantable devices has skyrocketed in the last decade

Corresponding Author: Rene Olivares-Navarrete, DDS, PhD, VCU College of Engineering, Department of Biomedical Engineering, 70 S. Madison Street, Room 3328, Richmond, VA 23220, ronavarrete@vcu.edu, 804-828-8718.

Declaration of interests

The authors declare that they have no known competing financial interests or personal relationships that could have appeared to influence the work reported in this paper.

and is expected to continue to grow worldwide [2]. Metals have been predominantly used in orthopedic and dental applications due to their mechanical properties (high strength/toughness and fatigue resistance) and biocompatibility [3–7]. Stainless steel (SS) has been used in bone applications for over a century for both temporary and permanent implants (*e.g.,* screws, nails, plates, pins) [8,9]. The most common SS used for implanted devices is low carbon 316L SS, which has increased corrosion resistance to improve biocompatibility [9]. Despite its good mechanical properties and wide use as biomaterial, SS does not promote tissue formation on the implant and lacks long-term biochemical stability [10–12]. Titanium (Ti) and Ti alloys have been widely used for orthopedic and dental applications due to their mechanical properties, low density, excellent biocompatibility, and chemical stability; the last two properties mainly result from the passivating oxide layer, spontaneously created on Ti and Ti alloys in contact with oxygen that provides the corrosion resistance needed for biomaterials exposed to the physiological environment [13–16]. Furthermore, Ti and Ti alloys allow the growth of bone formation in direct contact with the implanted material without forming a fibrous layer in a process known as osseointegration [16–18]. While Ti and Ti alloys have excellent biological responses, the difference between the modulus of Ti or Ti alloys and bone may lead to bone subsidence or stress shielding [19–21]. Polyetheretherketone (PEEK) was introduced as an alternative for Ti and Ti alloys due to its elastic modulus properties, which are relatively close to cortical bone. Additionally, its radiolucency allows observation of bone ingrowth into the implant using radiography [22,23]. While mechanical properties are more comparable to bone tissue, the biological response to PEEK favors the formation of fibrous tissue and reduces osteoblast differentiation resulting in severely reduced bone-to-implant contact [22,24–26]. The immune response of Ti, TiAlV, PEEK, and SS implants was our focus due to the varying degree of success and chronic inflammation associated with these materials in different tissue types [10,12,14,21,22,24,27,28]. SS, Ti, Ti alloys, and PEEK have been used widely in preclinical and clinical studies with varying success, it remains unclear why some biomaterials readily integrate with the surrounding bone while other biomaterials are encapsulated with fibrous tissue.

Implantation of biomaterials into the tissue results in an injury that releases danger-associated molecular patterns (DAMPs) from damaged cells and tissues and triggers an inflammatory response characterized by the infiltration and recruitment of immune cells to the injured tissue [26–28]. While innate and adaptive immune cells play significant roles in the initial inflammatory response and inflammatory process resolution, less is known about biomaterial characteristics affecting these processes and possible transition into a chronic inflammatory response and accumulation of granulation tissue [29,30]. Historically, most studies exploring the biological response to orthopedic and dental biomaterials have been focused on the effects of corrosion, wear particles, and molecule leaching. Still, it remains unclear whether the initial inflammatory response is affected by the implanted biomaterials [26,28,30,31]. We and others have demonstrated that surface characteristics of Ti and Ti alloy materials like surface roughness and hydrophilicity affect macrophage activation and polarization *in vitro* [32–37]. Furthermore, the local inflammatory process can be modulated by creating surface modifications to control macrophage behavior *in vivo* [32,35–37].

While macrophages play a fundamental role in controlling the inflammatory process and ablation reduces immune cell and mesenchymal stem cell (MSC) recruitment, other immune cells are equally important in initiating, amplifying, and resolving the inflammatory process after injury [31,32,35,38,39]. Neutrophils are the most abundant immune cells and the first to be recruited to the injury site [43–45]. Neutrophils destroy pathogens and clear wound debris in injured or inflamed tissues, restoring tissue homeostasis [43,44,46]. However, excessive neutrophil infiltration and activation at the injury site can cause collateral tissue damage through neutrophil degranulation and release of myeloperoxidase (MPO), neutrophil elastase (NE), matrix metalloproteases (MMPs), cytokines, and release of neutrophil extracellular traps (NETs) [43,44,46–48]. Altering biomaterial surface characteristics of the same bulk biomaterial alters neutrophil activation, with higher levels of MPO, NE, and NETs produced on smooth Ti surfaces than on rough-hydrophilic modifications [44]. However, whether neutrophils respond similarly to most biomaterials used for orthopedic and dental applications is unknown.

While macrophages and neutrophils participate in the early stages of the inflammatory response to implanted biomaterials, less is known about the role of T cells in response to implanted biomaterials. T cells are divided into two subclasses: helper $CD4^+$ T cells and cytotoxic $CD8^+$ T cells. While $CD8^+$ T cells generally interact directly with the target cell to induce apoptosis, $CD4^+$ T cells interact with different cell types through direct contact or indirect signaling through the release of cytokines. T cell activation requires recognition of the peptide-MHC complex by the T cell receptor, a costimulatory signal resulting from the interaction of CD28 on naïve T cells with antigen-presenting cells or B cells, and cytokines in the microenvironment that polarize T cells to specific phenotypes [49] Depending on the microenvironment stimuli, activated $CD4^+$ T cells may differentiate into diverse polarization states (Th1, Th2, Th17, Th22, Th9, or regulatory T cells (Treg)) with unique cytokine profiles and functions [50].

Th1 cells are crucial for host defense against intracellular pathogens and are responsible for certain organ-specific autoimmunity forms. Th1 cells can also activate macrophages through interferon-γ production [51]. Th2 cells mediate immune responses against extracellular parasites and are also responsible for allergic diseases. Th2 cells produce interleukins like IL-4 and IL-5 recruit other immune cells [52,53]. Th2 can induce alternatively activated macrophages or M2 phenotype by producing IL-4 and IL-13 [54]. Th17 orchestrates immune responses to extracellular pathogens and contributes to autoimmune disorders like multiple sclerosis, rheumatoid arthritis, and inflammatory bowel diseases [55,56]. Th17 cells produce IL-17A and IL-17F, which recruit and activate neutrophils and stimulate cells to produce inflammatory cytokines like IL-6 [57]. Treg cells play a fundamental role in maintaining immune tolerance and regulating the inflammatory and immunological response magnitude by controlling different cell types, including T cells [58].

Here we aim to elucidate the initial inflammatory response to four materials commonly used clinically for orthopedic and dental applications. Understanding the initial inflammatory response after biomaterial implantation and how biomaterial bulk chemistry may play a role in this process will allow us to better design biomaterial-specific modifications to enhance the immunomodulatory properties of implanted biomaterials.

2. Materials and Methods

2.1. Ti, TiAlV, PEEK, and SS disks, Implants and Material Characterization

Smooth 15 mm Ti, TiAlV, PEEK, and SS disks were provided by Institut Straumann AG (Basel, Switzerland). Ti disks were prepared from 1 mm thick grade 2 unalloyed Ti. Ti-aluminum-vanadium (TiAlV) disks were prepared from 1 mm thick grade 5 titanium-aluminum-vanadium alloy. Medical grade SS 316L disks were machined from a 15 mm rod to prepare disks with 1 mm thickness. Medical grade PEEK disks were machined from a 15 mm rod to prepare disks with 1 mm thickness. Ti, TiAlV, SS, and PEEK implants were machined from 5 mm rods to obtain 1 mm diameter rods. All materials were sterilized by γ-irradiation.

Surface roughness was assessed using confocal microscopy (LSM 910 Laser Scanning Microscope, Germany) with a 20x objective and a total measurement area of 798 μm × 798 μm. The arithmetic mean height of the scale limited surface (Sa) was calculated using a moving average Gaussian filter with a cut-off wavelength of 30 μm. Mean surface roughness was measured at six different areas of three samples for each surface type. A qualitative assessment of the surface was performed by scanning electron microscopy (SEM, Zeiss Auriga, Carl Zeiss, Germany). Surface hydrophilicity was assessed by sessile drop contact angle using a Ramé-Hart goniometer (Model 100–25a, Rame-Hart Instrument Co., Succasunna, NJ). Measurements using 1 μl drops of deionized water were performed at three locations per sample. Oxide layer composition was determined by X-ray photoelectron spectroscopy (XPS) using a PhI5000 VersaProbe spectrometer (ULVAC-PHI, Inc.) Spectra were acquired at a base pressure of 1×10–7 Pa using a focused scanning monochromatic Al-Ka source (1,486.6 eV) with a spot size of 200 μm. The instrument was run in the FAT analyzer mode. The pass energy used for survey scans was 187.85 eV and 46.95 eV for detail spectra. Data were analyzed using the program CasaXPS. The signals were integrated following Shirley background subtraction. Measurements were performed in three separate areas on each sample.

2.2. Mouse Femoral Implant

To assess the effect of biomaterial bulk composition on the local inflammatory cell phenotype, 12-week-old male C57BL/6 (Stock #000664) mice (The Jackson Laboratory, Bar Harbor, ME) were used for this study following a protocol approved by the Virginia Commonwealth University Institutional Animal Care and Use Committee. Mice were anesthetized using isoflurane delivered in O_2 gas and monitored for unconsciousness by pedal reflex. Mice were administered 1mg/kg buprenorphine SR LAB before surgical intervention. The skin overlaying the knee was dissected, and a longitudinal incision at one side of the patellar tendon was made. The patellar tendon was moved to expose the femoral condyles. A dental bur was used to access the medullary canal, and a 4 mm long cylindrical (Ø=1mm) Ti, Ti-Alloy, PEEK, or SS implant was then press fit, with placement confirmed by x-ray (n=6 mice per implant type). Animals were monitored until initial ambulation and every 24 hours afterward. All animals had access to food and water ad libitum for the duration of the study. No signs of infection were seen in this study.

On postoperative days 1, 3, or 7, mice were euthanized by CO_2 asphyxiation, and femoral bones were harvested. Time points were chosen based on previous work where we have identified changes in immune cell phenotypes, the amplification of the inflammatory signal, and the early resolution of the inflammatory stimuli [35,38–40,59]. To isolate peri-implant tissue, femurs were cut mid-shaft, and the implant and surrounding marrow were flushed using Accutase (Innovative Cell Technologies, San Diego, CA). To isolate implant-adherent cells, implants were incubated in Accutase for 20 minutes at 4°C. After detachment, cells were placed into two groups; 1) cells washed in PBS without calcium or magnesium for RNA isolation, or 2) washed with staining buffer (BioLegend, San Diego, CA) before staining for flow cytometry analysis as described below.

2.3. *Flow Cytometry for* in vivo *studies*

Single-cell suspensions from implant-adherent and peri-implant bone marrow were analyzed by flow cytometry. Before fluorescent staining, red blood cells were lysed with ACK lysis buffer (ThermoFisher Scientific, Waltham, MA). Next, Fc receptors were blocked by incubation with TruStain FcX (anti-CD16/32, BioLegend) to prevent the non-specific binding of subsequent fluorescent antibodies. Cell suspensions were then incubated with fluorescent antibodies to identify neutrophils ($CD45^+/CD11b^+/Ly6C^+/Ly6G^+$), macrophages ($CD45^+/CD11b^+/MHCII^+/F4/80^+$), pro-inflammatory macrophages ($Mac^+/CD80^+$), anti-inflammatory macrophages ($Mac^+/CD206^+$), T cells ($CD45^+/CD3^+$), $CD4^+$ T cells ($CD3^+/CD4^+$), and $CD8^+$ T cells ($CD3^+/CD8^+$), and mesenchymal stem cells ($CD45^-/SCA1^+/CD90^+/CD105^+$) (BioLegend). Samples were analyzed using a BD LSRFortessa-X20 Flow Cytometer (BD Biosciences, San Jose, CA) instrument with 200,000 events collected per sample. Results were analyzed using FlowJo v10 software (FlowJo LLC, Ashland, OR).

2.4. Gene Expression

mRNA was extracted from cells isolated from implant-adherent and peri-implant cells using TRIzol (ThermoFisher), and 1ug of RNA was converted to cDNA using the iScript cDNA synthesis kit (BioRad, Hercules, CA). qPCR was performed using SsoAdvanced Universal SYBR green supermix (Bio-Rad) to assess mRNA expression of inflammatory molecules (*Il1b, Il6, Il10, Il12, Il17a, Tnf, Arg1, Nos2, Tgfb1*) and osteogenic associated genes (*Runx2, Sp7, Bglap*) using pre-designed primers PrimePCR™ (BioRad). Differences were determined by 2-ΔΔCT analysis calculated using endogenous housekeeping gene (Rsp18) and respective controls.

2.5. Neutrophil Isolation

12-week-old male C57BL/6J mice (Stock #000664, Jackson Laboratory) were used for neutrophil isolation. Mice were euthanized by CO_2 asphyxiation followed by cervical dislocation. Bone marrow was flushed from the femoral medullary canal with phosphate-buffered saline PBS. Erythrocytes were removed from the marrow isolate using ACK Lysing Buffer. Neutrophils were then isolated by centrifugation using Histopaque 1077 and 1119 (Sigma-Aldrich, St. Louis, MO) [40]. Viability and purity were confirmed by flow cytometry. Following pretreatment with anti-CD16/32 to prevent non-specific fluorescence,

viable (Zombie NIR, BioLegend) neutrophils were identified as described above. A purity of approximately 95% was obtained for each experiment.

2.6. Neutrophil Response to Biomaterials

To evaluate the neutrophil response to the different biomaterials, neutrophils were seeded on Ti, TiAlV, PEEK, or SS disks at a density of 200,000 cells/cm^2 (n=6) and cultured with RPMI 1640 (ThermoFisher) supplemented with 10% fetal bovine serum (ThermoFisher), 50U/mL penicillin-50 μg/mL streptomycin (ThermoFisher) for 4 hours. After incubation, conditioned media was harvested, and levels of neutrophil elastase, myeloperoxidase, and MCP-1 were measured by enzyme-linked immunoassay (ELISA, R&D Systems, Minneapolis, MN). Neutrophil extracellular trap production in response to biomaterials was assessed by detecting MPO-DNA complexes using a modified sandwich ELISA described previously [46,59]. Anti-MPO monoclonal antibody (R&D Systems, Minneapolis, MN) was used as a capture antibody (1 μg/mL) in a 96-well microplate. A peroxidase-labeled anti-DNA monoclonal antibody (capture antibody of commercial Cell Death Detection ELISA kit; Roche, Mannheim, Germany) was used as a detection antibody according to the manufacturer's instructions. Absorbance at 405 nm was measured using Synergy HTX Multi-Mode Reader (BioTek, Winooski, VT).

2.7. Macrophage isolation

Bone marrow-derived macrophages were isolated from the femurs of 12-week-old male C57BL/6 mice (The Jackson Laboratory) as previously described [35–40]. Briefly, bone marrow cells were flushed from the femurs using DPBS (ThermoFisher). Red blood cells were removed from flushed bone marrow by adding ACK Lysing Buffer (ThermoFisher). Cells were counted and plated in 175 cm^2 flasks at a density of 500,000 cells/mL in 30mL RPMI 1640 (ThermoFisher) supplemented with 10% fetal bovine serum (ThermoFisher), 50U/mL penicillin-50 μg/mL streptomycin (ThermoFisher), and 30ng/mL macrophage colony-stimulating factor (M-CSF, BioLegend). Cells were cultured at 37°C, 5% CO_2, and 100% humidity. New media supplemented with M-CSF was added after four days. After seven days of incubation with M-CSF, macrophages were passaged with Accutase (ThermoFisher) at room temperature for 1 hour for experiments.

2.8. Macrophage response to biomaterials

To evaluate macrophage activation on the Ti, TiAlV, PEEK, and SS surfaces (n=6), naïve macrophages were plated on the different biomaterials at 100,000 cells/cm^2. After 24 hours of incubation, conditioned media were collected, and secreted pro-inflammatory cytokines (IL1β, IL6, and TNFα), anti-inflammatory interleukins (IL4 and IL10), and MCP-1 (BioLegend) were quantified by ELISA based on manufacturer's protocol. Protein secretion was normalized to DNA content measured in cell lysate (Quant-IT™ PicoGreen dsDNA Assay, ThermoFisher).

2.9. Neutrophil-directed Macrophage Polarization

To evaluate whether neutrophil activation in response to the different biomaterials induces macrophage polarization, neutrophils were cultured at a density of 200,000 cells/cm^2 for

4 hours on Ti, TiAlV, PEEK, and SS surfaces (n=6). After incubation, naïve macrophages were added directly to the neutrophils on the different biomaterials at a density of 100,000 cells/cm^2, and the cells were co-cultured for 24 hours. Finally, cells were detached into single-cell suspension with Accutase (ThermoFisher) as previously described. Polarization of macrophages was characterized as pro-inflammatory macrophages (CD11b$^+$/F4/80$^+$/CD80$^+$/CD206$^-$) and anti-inflammatory macrophages (CD11b$^+$/F4/80$^+$/CD206$^+$/CD80$^-$) (BioLegend) using flow cytometry. Samples were analyzed using a BD LSRFortessa-X20 Flow Cytometer (BD Biosciences) instrument with 50,000 events collected per sample. Results were analyzed using FlowJo v10 software (FlowJo).

2.10. Neutrophil-directed Macrophage Recruitment

Macrophage recruitment in response to neutrophil activation on different biomaterials was assessed by pre-labeling naïve macrophages with CellTracker Green CMFDA (ThermoFisher), then 50,000 cells were plated in serum-free RPMI 1640 (ThermoFisher) in 8 μm pores transwell inserts. Neutrophils seeded at 200,000 cells/cm2 on Ti, TiAlV, PEEK, and SS disks (n=6) were on the bottom of the transwell plate. Cells were incubated together for 24 hours, and after incubation, inserts were discarded, and cells were washed twice with warm PBS. Fluorescence intensity, at 490/520 excitation/emission (nm) in the lower chamber, was used to measure recruited labeled cells using Synergy HTX Multi-Mode Reader (BioTek).

2.11. Macrophage-directed T helper cell polarization

The effect of macrophage response to the different biomaterials in polarizing T helper cells was explored using direct co-cultures. Naïve macrophages were cultured on Ti, TiAlV, PEEK, or SS disks (n=6) for 24 hours at a density of 100,000 cells/cm^2. After incubation, activated CD4$^+$ T cells (Dynabeads™, CD3/CD28, ThermoFisher) were added to the culture in a 1:1 ratio, and macrophages and T cells were allowed to interact for additional 24 hours. After 24 hours of interaction, cells were collected and analyzed by flow cytometry. Changes in T helper subsets were determined as follows: Th1 (CD4$^+$/Tbet$^+$), Th2 (CD4$^+$/Gata3$^+$), Th17 (CD4$^+$/Rorγt$^+$), and Treg (CD4$^+$/FoxP3$^+$) (BioLegend). Samples were analyzed using a BD LSRFortessa-X20 Flow Cytometer (BD Biosciences) instrument with 50,000 events collected per sample. Results were analyzed using FlowJo v10 software (FlowJo).

2.12. Data Analysis

Data are presented as mean ± SD of n=6 independent cultures per variable. Statistical analysis was performed using Prism9 (GraphPad Software, San Diego, CA). Data were first subjected to the Shapiro-Wilk normality test. Results from this test indicated that the data were normally distributed. A one-factor, equal analysis of variance (ANOVA) was used to test the null hypothesis that group means were equal at a significance level of α=0.05, with post hoc Tukey's HSD test for multiple comparisons.

3. Results

3.1 Biomaterial Characterization

Scanning electron microscopy images showed that all substrates were smooth, with some irregularities observed in Ti, TiAlV, and PEEK. However, these minor irregularities did not create significant surface morphology or roughness differences (Figure 1A). All samples analyzed have similar quantitative surface roughness Ti (Sa= 0.76 μm), TiAlV (Sa= 0.73 μm), PEEK (Sa= 0.71 μm), and SS (Sa= 0.62 μm). Water contact angle measurements (Figure 1B) showed that the most hydrophobic surface was rough TiAlV (92.6°), followed by Ti (88.6°), PEEK (85.6°), and SS (72.2°). Surface composition showed the presence of titanium, oxygen, carbon, and nitrogen in the Ti oxide layer; titanium, oxygen, carbon, aluminum, and vanadium in the TiAlV oxide layer; oxygen, carbon, chromium, iron, and molybdenum in the SS oxide layer; and carbon and oxygen in PEEK surface (Figure 1C).

3.2 *Orthopaedic Biomaterials Recruit Differentially Immune Cell* In vivo

To understand the effect of implants with different biomaterial compositions on the temporal immune cell response, we implanted Ti, TiAlV, PEEK, and SS rods intramedullary in mice for 1, 3, and 7 days. On day 1 post-implantation (Figure 2A), SS and PEEK recruited higher levels of neutrophils but fewer T cells than Ti and TiAlV. Macrophage recruitment was highest on Ti. There were no differences in the levels of pro- or anti-inflammatory macrophages or $CD4^+$ or $CD8^+$ T cells between the different biomaterials. Levels of MSCs were minimal, with no differences between the groups. By day 3 post-implantation (Figure 3A), neutrophils remained higher in TiAlV, PEEK, and SS compared to Ti implants. Total macrophage recruitment was the highest on Ti implants. Immunophenotyping of total macrophages showed higher recruitment of pro-inflammatory macrophages in PEEK and SS implants than Ti and TiAlV. In contrast, the recruitment of anti-inflammatory macrophages was higher on Ti than on TiAlV, PEEK, and SS. T cell recruitment was higher in PEEK and SS, with the lowest levels observed in Ti implants. $CD4^+$ T cells were elevated in PEEK, SS, and TiAlV, with the lowest levels in Ti implants. $CD8^+$ T cells were similar in all biomaterials. MSCs recruitment was higher on Ti and TiAlV than PEEK and SS. On day 7 (Figure 4A), neutrophils remained high in PEEK and SS, while neutrophils were lowest on Ti implants. Pro-inflammatory macrophages were elevated in PEEK and SS and the lowest in Ti implants. Anti-inflammatory macrophages were the highest in TiAlV and lower in PEEK and SS implants compared to Ti implants. Total T cells and $CD4^+$ T cells were higher in PEEK and SS and lowest in Ti implants. $CD8^+$ T cells were slightly higher in PEEK and SS than Ti and TiAlV. MSCs recruitment was the highest in Ti and the lowest in PEEK implants.

3.3 Inflammatory Genes are Differentially Expressed in Implant-Adherent Cells in Response to Different Orthopaedic Biomaterials

To understand the effect of implants with different biomaterial compositions on the temporal inflammatory response, we analyzed the temporal gene expression from implant-adherent cells implanted at 1, 3, and 7 days. On day 1 (Figure 2B), we observed higher expression of pro-inflammatory genes (*Il1b, Il6, Il12, Il17a, Tnf, Nos2*) in TiAlV, PEEK, and SS and lower *Il10* and *Arg1* when compared to Ti implants. Cells on PEEK implants expressed

the highest levels of *Il6*, *Il12*, and *Nos2,* while cells on Ti implants expressed the highest *Arg1*. Expression of osteogenic-related genes was not detected in any of the groups. On day 3 (Figure 3B), expression of pro-inflammatory genes increased in all groups with higher levels on TiAlV, PEEK, and SS compared to Ti implants. Cells on Ti implants expressed the highest levels of *Il10* and *Arg1* and the lowest levels of *Il1b, Il6, Il12, Il17a, Tnf,* and *Nos2.* Expression of osteogenic genes was not detected at this time point. Finally, gene expression of *Il1b, Il6, Il10, Il12, Il17a, Tnf*, and *Nos2* was higher on PEEK and SS at day 7 post-implantation when compared to Ti and TiAlV (Figure 4B). Osteogenic genes and *Tgfb1* were expressed the most in Ti implants and the lowest in PEEK implants.

3.4 PEEK and 316L Stainless Steel Increase MPO, NE, and NET Formation

We next sought to examine the effect of biomaterial chemistry on neutrophil activation, degranulation, and NET formation on Ti, TiAlV, PEEK, or SS. The secretion of NE and MPO as a product of degranulation in neutrophils was the highest in PEEK substrates and the lowest in Ti in cell culture supernatants (Figure 5). Furthermore, levels of MCP-1 chemokine were higher on PEEK and SS than on Ti and TiAlV substrates. Finally, NET formation was lower on Ti than on TiAlV, PEEK, and SS (Figure 5).

3.5 Macrophages Cultured on PEEK and SS Produce Higher Pro-Inflammatory Microenvironment

Inflammatory cytokine production was assessed bone marrow-derived macrophages cultured on Ti, TiAlV, PEEK, or SS. Secretion of pro-inflammatory cytokines IL-1β, IL-6, and TNF-α was higher on TiAlV, PEEK, and SS when compared to Ti substrates (Figure 6). Macrophages cultured on PEEK substrates produced the greatest IL-1β and TNF-α and the lowest IL-1β and TNF-α levels on Ti substrates. Macrophages on Ti substrates produced the highest anti-inflammatory interleukins IL-4 and IL-10. MCP-1, a potent macrophage chemoattractant, levels were higher on PEEK and SS and the lowest in Ti substrates (Figure 6).

3.6 Neutrophil Response to PEEK and SS Increased Polarization of Macrophages into a Pro-Inflammatory Phenotype and Macrophage Chemotaxis in a Co-Culture Model

Next, we explored how activation of neutrophils by the different biomaterials alters naïve macrophage polarization and migration in direct and indirect co-culture models. Direct neutrophil-macrophage co-cultures on TiAlV, PEEK, and SS polarized more macrophages into a pro-inflammatory phenotype than Ti (Figure 7A). Anti-inflammatory macrophages were the highest in Ti and TiAlV and the lowest in PEEK substrates. Indirect neutrophil-macrophage co-cultures were performed to assess neutrophil-directed macrophage chemotaxis. Neutrophils cultured on PEEK and SS induced higher macrophage recruitment than neutrophils in Ti or TiAlV (Figure 7B). The lowest macrophage recruitment was observed in neutrophils cultured on Ti substrates.

3.7 Macrophage Response to PEEK and SS Increased CD4$^+$ T cell Polarization towards Th1 and Th17

To evaluate if macrophage response to orthopedic biomaterials induces CD4$^+$ T cell Polarization, we performed direct macrophage-T cell co-cultures. Macrophages cultured on PEEK and SS caused higher Th1 and Th17 polarization than macrophages cultured on Ti or TiAlV substrates (Figure 8). On the other hand, macrophages cultured on PEEK and SS induced lower Th2 and Treg polarization than Ti and TiAlV. Macrophages cultured on Ti substrates caused the highest Th2 and Treg polarization (Figure 8).

4. Discussion

Biomaterials used for orthopedic and dental applications are biocompatible and, in many cases, result in osseointegration of the implanted biomaterial. Previously, we have shown that the initial inflammatory response and immune cell activation after biomaterial implantation depend on biomaterial surface characteristics [35–40,44]. We and others have demonstrated that macrophages respond differentially to changes in Ti surface properties such as roughness and hydrophilicity [35–40]. Considering this, we used materials with similar surface roughness and wettability to isolate the effect of material composition on the inflammatory response. While implants with a roughened surface have become the standard for osseointegrated implants, we tested only smooth materials in this study to isolate the effect of chemical composition on the inflammatory response. This work found that implant composition affected the immune cell and inflammatory response to biomaterials commonly used in orthopedics and dentistry.

Neutrophils are the first cells to be recruited at the site of the injury, and in the case of biomaterial implantation, to the implantation site [45]. While the role of neutrophils in disease is known, the response of neutrophils to biomaterials remains unclear. In sterile inflammation, DAMPs, interleukins, and lipid inflammatory mediators are released by damaged cells and tissues, chemoattracting neutrophils to the injury site where they produce inflammatory mediators, proteolytic enzymes, NETs, and generate reactive oxygen species [44–46,60]. The neutrophil-driven inflammatory response is essential for eliminating possible pathogens and clearing debris from injury, tissue damage, or biomaterial implantation [61–65]. However, excessive neutrophil activation and degranulation, NET formation, or persistent presence of activated neutrophils in the injury site can cause further damage and harm surrounding tissues [66,67] This study found fewer peri-implant neutrophils with Ti implants than with PEEK, SS, or TiAlV implants.

We previously reported higher NET formation on smooth Ti surfaces than rough or rough-hydrophilic Ti modifications [44]. In this work, we found that although smooth Ti activates neutrophils and induces a pro-inflammatory response, PEEK, SS, and TiAlV induce more robust neutrophil activation and more NET formation. We found that neutrophil presence remained elevated in PEEK, SS, and TiAlV implants at seven days post-implantation, suggesting that Ti implants resolve the inflammatory response more quickly. We also found higher macrophage recruitment in peri-implant tissue around PEEK, SS, and TiAlV implants compared to Ti implants at seven days. Our *in vitro* studies showed that neutrophils cultured on PEEK and SS produced higher levels of MCP-1 than Ti or TiAlV, suggesting

potentially more recruitment of monocytes/macrophages. This was confirmed in an *in vitro* chemotaxis model where neutrophils were seeded on Ti, TiAlV, PEEK, or SS substrates, and macrophages were seeded in a transwell. In addition, macrophage recruitment was higher when neutrophils were cultured on PEEK, SS, and TiAlV, confirming that MCP-1 is a good predictor of macrophage recruitment to the implantation site. MCP-1 or chemokine C-C ligand 2 (CCL2) is a potent chemotactic factor for monocytes, circulating macrophages, and neutrophils [68]. Our *in vivo* results also demonstrated that PEEK and SS implants polarized more macrophages into a pro-inflammatory phenotype than Ti and TiAlV at day 3. However, TiAlV implants had higher levels of pro-inflammatory macrophages at day 7 post-implantation compared to Ti implants.

Biomaterial parameters including chemical composition, porosity, surface roughness, wettability, and stiffness can alter macrophage phenotype [35–40,69,70]. Still, the biological mechanisms that govern macrophage polarization in response to these parameters are unknown. Here, we investigate if the neutrophil response to Ti, TiAlV, PEEK, or SS can polarize macrophages to a pro- or anti-inflammatory phenotype in a direct co-culture model mimicking the cellular dynamics after biomaterial implantation with neutrophils early recruited to the biomaterial and then macrophages recruited by neutrophils. Macrophages were polarized into a pro-inflammatory phenotype to the greatest degree and to the least degree into an anti-inflammatory phenotype when interacting with neutrophils seeded on PEEK substrates. Macrophages also were more pro-inflammatory when co-cultured with neutrophils seeded on SS or TiAlV substrates than on Ti. We attribute the pro-inflammatory macrophage polarization in our co-culture model to the stronger neutrophil response to PEEK and SS, resulting in higher levels of NE, MPO, and NET formation. Previously, we demonstrated that neutrophils produce different stimuli to polarize macrophages, including interleukins, cytokines, NE, MPO, and NETs [44]. While these signals contribute to the inflammatory macrophage phenotype, NET formation is perhaps the stronger signal for macrophage pro-inflammatory polarization since pharmacological inhibition of NET formation significantly reduces levels of pro-inflammatory macrophages [44]. The release of NETs by neutrophils also releases NE and MPO and generates reactive oxygen species, all of which have a pro-inflammatory effect on macrophages [71–73]. These results showed that neutrophils are fundamental for recruiting and activating macrophages and that pro-inflammatory macrophage polarization strongly correlates with high levels of MPO, neutrophil elastase, and NET formation.

Our *in vitro* macrophage studies also demonstrate that even in the absence of neutrophils, macrophages are sensitive to changes in surface chemistry and, similarly to neutrophils, produce higher levels of pro-inflammatory cytokines on PEEK, SS, and TiAlV compared to Ti substrates. Furthermore, the same biomaterials generated lower levels of anti-inflammatory interleukins than Ti substrates. Here, it should be noted that the immune response to biomaterial implantation is not solely driven by material choice or physiochemical modification. Instead, the immune response is a cumulative response to the tissue damage during the surgical procedure and the biomaterial response. Furthermore, there is a degree of variability in the immune response between individuals and species. The presence of bacteria and pathogen-associated molecular patterns will also alter the initial inflammatory response [74–77]. This is mainly observed in dental implants where

toll-like receptors and other pattern-recognition receptors can recognize constituents from the oral microbiota to initiate an inflammatory response [78]. Peri-implant mucositis and peri-implantitis are implant-related infections. Peri-implantitis is an inflammatory process affecting both soft and hard tissues surrounding an osseointegrated implant, increasing the risk of late implant failure [79–81].

The scope of this work was to investigate the effect of different biomaterial compositions on immune cell response and their inflammatory response. While there is not a single study comparing the macrophage response to the biomaterials we used in this study, some studies have independently examined macrophage response to PEEK, SS, or TiAlV. PEEK is generally used for craniofacial and orthopedic applications due to chemical stability, radiolucency, and excellent mechanical properties [22].

Local inflammation, extended inflammation after biomaterial implantation or after implant osseointegration, may lead to implant failure. Aseptic implant loosening has been recently attributed to macrophage recruitment and phagocytosis in response to wear particles [82,83]. In a prior study, macrophages were exposed to polymethylmethacrylate (PMMA) particles, which promote macrophage secretion of TNF-α, stimulating osteoblast production of IL-6 and other pro-inflammatory factors [83]. In our study, we have demonstrated higher production of both TNF-α and IL-6 by macrophages on TiAlV, PEEK, and SS surfaces. These cytokines promote higher recruitment of macrophages to the bone-implant microenvironment, as well as increased osteoclastogenesis, resulting in bone resorption that will lead to implant loosening [82,83]. These cellular processes ultimately impact osseointegration, and the increased inflammatory response to biomaterials like PEEK and SS inhibits bone formation and promotes bone resorption [84]. While acute inflammation after biomaterial implantation is normal and needed to start the tissue remodeling and regenerative process, chronic inflammation at the implant site results in insufficient implant integration [84–88]. PEEK implants generally have poor osseointegration and produce foreign body responses resulting in fibrous encapsulation [26,27,84]. Other studies have found macrophage infiltration and formation of foreign body giant cells adjacent to the implant several months after implantation [26,85]. Recently, a study comparing the soft tissue response to dental implant closure caps made of PEEK or Ti found that multinucleated giant cells were present in caps made of both materials; however, the number of multinucleated giant cells was significantly higher on caps made of PEEK [28]. Macrophage-like cells activate into a pro-inflammatory state in response to unmodified PEEK substrates, and surface modifications in PEEK that increase surface roughness attenuate the inflammatory response and increase osseointegration [89]. PEEK osseointegration can also be improved by increasing surface topography, either by roughening the surface or by titanium or hydroxyapatite coatings [90–92]. However, others have suggested that surface chemistry contributes to macrophage response and foreign body giant cell formation in response to biomaterials [93]. Macrophage polarization is sensitive to changes in the oxide layer composition on Ti materials, where substrates and implants with the same surface roughness but with different hydrophilicity differentially polarize macrophages to the more pro-inflammatory phenotype observed on hydrophobic Ti and more anti-inflammatory macrophages on hydrophilic Ti in vitro and in vivo [37,39].

Macrophage polarization affects and amplifies T-cell polarization. For example, we have reported stronger Th1 and Th17 polarization in response to smooth and rough Ti compared to rough-hydrophilic Ti substrates, which polarizes T cells towards a Th2 and Treg phenotype [39]. Here, we found low T-cell infiltration in vivo one day following implantation. However, T cells rapidly increased in the peri-implant tissue by three days post-implantation on all materials tested. Recruitment of $CD4^+$ and $CD8^+$ T cells was higher in animals receiving PEEK or SS implants at 3 and 7 days, compared to Ti and TiAlV implants.

Interestingly, while Ti and TiAlV implants showed an increase in T cells by day 3, these levels decreased by day 7, suggesting a resolution of the inflammatory response. This suggested resolution of the inflammatory response was not observed in response to PEEK and SS, where T cells, neutrophils, and pro-inflammatory macrophages remained elevated after seven days post-implantation. This T cell response was similarly observed in different study analyzing the immune response to copper, PEEK, or Ti implantation in rabbit tibia after at 10- and 28-days [41,42]. This study found that PEEK implants induced higher immune cell activation than Ti that remained elevated at 28 days post-implantation, including $CD4^+$ T cells that increased from day 10 to day 28, concluding that PEEK implants induce a prolonged inflammatory phase [42]. While it is known that T cells participate actively during immune responses against pathogens, their role in response to implanted biomaterials remains unclear. Besides their role in fighting pathogens, T cells are also involved in fibrotic responses such as pulmonary fibrosis and liver fibrosis [94,95]. Some studies suggest that T cells mediate macrophage fusion and foreign body giant cell formation when early T cell recruitment occurs after biomaterial implantation [59]. The rate of monocyte/macrophage fusion and formation of foreign body giant cells increased by 60% when T cells are present during the initial monocyte/macrophage interaction with biomaterials, compared to monocytes/macrophages in the absence of T cells [96]. The same study observed that T cells could adhere to the biomaterial, but 90% of the T cells were associated with adherent macrophages [96]. Our study identified T cells in peri-implant tissue at the earliest time point measured (1 day), which peaked at three days post-implantation. Surface chemistry and hydrophilicity of biomaterials affect $CD4^+$ T cell adhesion and alter cytokine secretion [97,98].

Moreover, $CD4^+$ T cells are present in the fibrotic capsule surrounding implants [99,100] and in pro-regenerative materials and Ti during osseointegration [39,101]. In this regard, Th17 cells have been identified in large amounts surrounding breast implants, and their presence correlates with the expression of *Col1a1* and *Tgfb1* gene expression [100]. Another study assessing the composition of lymphocytes in the fibrous capsule of breast implant found the predominance of $CD4^+$ T cells with the production of IL-17, IL-6, IL-8, and IFN-γ, suggesting a Th1/Th17 local immune response [99]. The same study also observed an inverse correlation between the severity of the fibrotic tissue and the number of $CD4^+$ Treg present in fibrotic tissue, suggesting that the presence of $CD4^+$ Treg cells at early stages post-implantation may delay or abolish fibrous encapsulation [99]. In another study, tissue-derived biomaterial scaffolds enhance the development of a pro-regenerative immune environment through modulation of the inflammatory microenvironment by Th2 cells and reduction of Th1/Th17 response [101]. We have also previously shown that macrophage

response to rough-hydrophilic skews $CD4^+$ T cell polarization towards Th2/Treg phenotype and reduces Th1/Th17 polarization [39]. Results from our macrophage-T cell co-cultures showed that PEEK and SS favor Th1/Th17 polarization and decrease Th2/Treg polarization suggesting that PEEK and SS produce a microenvironment more conducive to fibrous encapsulation or foreign body response.

5. Conclusion

Our results, summarized in figure 9, demonstrate that Ti, TiAlV, PEEK, and SS produce a differential inflammatory response *in vivo*, and our *in vitro* studies using single cell type culture. Co-cultures confirmed immune cells respond differently to Ti, TiAlV, PEEK, and SS. Pure Ti produced the least inflammatory response and immune cell activation *in vitro* and *in vivo*, while PEEK and SS produced robust inflammatory responses that may lead to fibrous encapsulation.

Supplementary Material

Refer to Web version on PubMed Central for supplementary material.

Acknowledgments

Research reported in this publication was supported by the National Institute of Dental and Craniofacial Research of the National Institutes of Health under award number R01DE028919. The content is solely the responsibility of the authors and does not necessarily represent the official views of the National Institutes of Health. Institut Straumann AG, Basel, Switzerland, provided Ti, TiAlV, PEEK, and SS disks and implants. Services in support of the research project were provided by the VCU Massey Cancer Center Flow Cytometry Shared Resource supported, in part, with funding from NIH-NCI Cancer Center Support Grant P30 CA016059

References

[1]. Brittain R, Howard P, Lawrence S, Stonadge J, Wilkinson M, Wilton T, Dawson-Bowling S, Watts A, Esler C, Goldberg A, Jameson S, Jennison T, Toms A, Young E, Boulton C, Taylor D, Espinoza O, Mccormack V, Newell C, Royall M, Swanson M, Ben-Shlomo Y, Blom A, Clark E, Deere K, Gregson C, Judge A, Lenguerrand E, Price A, Prieto-Alhambra D, Rees J, Sayers A, Whitehouse M, NJR statistical analysis, support and associated services, National Joint Registry | 18th Annual Report. 3 (n.d.).

[2]. Elani HW, Starr JR, Da Silva JD, Gallucci GO, Trends in Dental Implant Use in the U.S., 1999–2016, and Projections to 2026, J Dent Res. 97 (2018) 1424–1430. 10.1177/0022034518792567. [PubMed: 30075090]

[3]. Fathi MH, Doostmohammadi A, Bioactive glass nanopowder and bioglass coating for biocompatibility improvement of metallic implant, J Mater Process Technol. 209 (2009) 1385–1391. 10.1016/J.JMATPROTEC.2008.03.051.

[4]. Merritt K, Brown SA, Release of hexavalent chromium from corrosion of stainless steel and cobalt—chromium alloys, J Biomed Mater Res. 29 (1995) 627–633. 10.1002/JBM.820290510. [PubMed: 7622548]

[5]. Saleh MM, Saleh MM, Touny AH, Al-Omair MA, Biodegradable/biocompatible coated metal implants for orthopedic applications, Biomed Mater Eng. 27 (2016) 87–99. 10.3233/BME-161568. [PubMed: 27175470]

[6]. Hornberger H, Manaranche C, Corrosion and biocompatibility of dental alloys, Eur Cell Mater. 9 (2005) 35–36. https://www.researchgate.net/publication/268337962 (accessed October 23, 2022).

[7]. Haslauer CM, Springer JC, Harrysson OLA, Loboa EG, Monteiro-Riviere NA, Marcellin-Little DJ, In vitro biocompatibility of titanium alloy discs made using direct metal fabrication, Med Eng Phys. 32 (2010) 645–652. 10.1016/J.MEDENGPHY.2010.04.003. [PubMed: 20447856]

[8]. Bekmurzayeva A, Duncanson WJ, Azevedo HS, Kanayeva D, Surface modification of stainless steel for biomedical applications: Revisiting a century-old material, Materials Science and Engineering: C. 93 (2018) 1073–1089. 10.1016/J.MSEC.2018.08.049. [PubMed: 30274039]

[9]. Virtanen S, Milošev I, Gomez-Barrena E, Trebše R, Salo J, Konttinen YT, Special modes of corrosion under physiological and simulated physiological conditions, Acta Biomater. 4 (2008) 468–476. 10.1016/J.ACTBIO.2007.12.003. [PubMed: 18226986]

[10]. Al-Mamun NS, Mairaj Deen K, Haider W, Asselin E, Shabib I, Corrosion behavior and biocompatibility of additively manufactured 316L stainless steel in a physiological environment: the effect of citrate ions, Addit Manuf. 34 (2020) 101237. 10.1016/J.ADDMA.2020.101237.

[11]. Yanlong X, Lei Z, Yongfeng S, Ning L, Yongli L, Bin L, Qinghua X, Chaoliang H, Xuesi C, Surface Modification of 316L Stainless Steel by Grafting Methoxy Poly(ethylene glycol) to Improve the Biocompatibility, Chem. Res. Chin. Univ. (2015) 651–657. 10.1007/s40242-015-5027-0.

[12]. Gao J, Cao Y, Ma Y, Zheng K, Zhang M, Hei H, Gong H, Yu S, Kuai P, Liu K, Wear, Corrosion, and Biocompatibility of 316L Stainless Steel Modified by Well-Adhered Ta Coatings, J Mater Eng Perform. (2022) 1–15. 10.1007/S11665-022-06928-9/FIGURES/12.

[13]. Larsson C, Thomsen P, Lausmaa J, Rodahl M, Kasemo B, Ericson LE, Bone response to surface modified titaniumlimplants: studies on electropolished implants with different oxide thicknesses and morphology, (n.d.).

[14]. Okazaki Y, Ito Y, Kyo K, Tateishi T, Corrosion resistance and corrosion fatigue strength of new titanium alloys for medical implants without V and Al, Materials Science and Engineering: A. 213 (1996) 138–147. 10.1016/0921-5093(96)10247-1.

[15]. Czarnowska E, Wierzchoń T, Maranda-Niedbała A, Properties of the surface layers on titanium alloy and their biocompatibility in in vitro tests, J Mater Process Technol. 92–93 (1999) 190–194. 10.1016/S0924-0136(99)00228-9.

[16]. Möller B, Terheyden H, Ail Y, Purcz NM, Hertrampf K, Tabakov A, Behrens E, Wiltfang J, A comparison of biocompatibility and osseointegration of ceramic and titanium implants: an in vivo and in vitro study, Int J Oral Maxillofac Surg. 41 (2012) 638–645. 10.1016/J.IJOM.2012.02.004. [PubMed: 22406235]

[17]. Sul YT, Kang BS, Johansson C, Um HS, Park CJ, Albrektsson T, The roles of surface chemistry and topography in the strength and rate of osseointegration of titanium implants in bone, J Biomed Mater Res A. 89A (2009) 942–950. 10.1002/JBM.A.32041.

[18]. Carlsson L, Röstlund T, Albrektsson B, Albrektsson T, Brånemark P-I, Acta Orthopaedica Scandinavica Osseointegration of titanium implants, (2009). 10.3109/17453678608994393.

[19]. Huiskes R, Weinans H, van Rietbergen B, The relationship between stress shielding and bone resorption around total hip stems and the effects of flexible materials, Clin Orthop Relat Res. (1992) 124–134.

[20]. Chen Y, Chen D, Guo Y, Wang X, Lu X, He Z, Yuan W, Subsidence of titanium mesh cage: A study based on 300 cases, J Spinal Disord Tech. 21 (2008) 489–492. 10.1097/BSD.0B013E318158DE22. [PubMed: 18836360]

[21]. Campbell PG, Cavanaugh DA, Nunley P, Utter PA, Kerr E, Wadhwa R, Stone M, PEEK versus titanium cages in lateral lumbar interbody fusion: a comparative analysis of subsidence, Neurosurg Focus. 49 (2020) E10. 10.3171/2020.6.FOCUS20367.

[22]. Kurtz SM, Devine JN, PEEK biomaterials in trauma, orthopedic, and spinal implants, Biomaterials. 28 (2007) 4845–4869. 10.1016/J.BIOMATERIALS.2007.07.013. [PubMed: 17686513]

[23]. Schwitalla AD, Abou-Emara M, Spintig T, Lackmann J, Müller WD, Finite element analysis of the biomechanical effects of PEEK dental implants on the peri-implant bone, J Biomech. 48 (2015) 1–7. 10.1016/J.JBIOMECH.2014.11.017. [PubMed: 25435385]

[24]. Olivares-Navarrete R, Hyzy SL, Slosar PJ, Schneider JM, Schwartz Z, Boyan BD, Implant Materials Generate Different Peri-implant Inflammatory Factors: Poly-ether-ether-ketone

Promotes Fibrosis and Microtextured Titanium Promotes Osteogenic Factors, Spine (Phila Pa 1976). 40 (2015) 399. 10.1097/BRS.0000000000000778. [PubMed: 25584952]

[25]. Olivares-Navarrete R, Hyzy SL, Gittens I RA, Schneider JM, Haithcock DA, Ullrich PF, Slosar PJ, Schwartz Z, Boyan BD, Rough titanium alloys regulate osteoblast production of angiogenic factors, The Spine Journal. 13 (2013) 1563–1570. 10.1016/J.SPINEE.2013.03.047. [PubMed: 23684238]

[26]. Nieminen T, Kallela I, Wuolijoki E, Kainulainen H, Hiidenheimo I, Rantala I, Amorphous and crystalline polyetheretherketone: Mechanical properties and tissue reactions during a 3-year follow-up, J Biomed Mater Res A. 84 (2008) 377–383. 10.1002/JBM.A.31310. [PubMed: 17618477]

[27]. Wu SH, Li Y, Zhang YQ, Li XK, Yuan CF, Hao YL, Zhang ZY, Guo Z, Porous titanium-6 aluminum-4 vanadium cage has better osseointegration and less micromotion than a poly-ether-ether-ketone cage in sheep vertebral fusion, Artif Organs. 37 (2013). 10.1111/AOR.12153.

[28]. Caballé-Serrano J, Chappuis V, Monje A, Buser D, Bosshardt DD, Soft tissue response to dental implant closure caps made of either polyetheretherketone (PEEK) or titanium, Clin Oral Implants Res. 30 (2019) 808–816. 10.1111/CLR.13487. [PubMed: 31125452]

[29]. Sadtler K, Wolf MT, Ganguly S, Moad CA, Chung L, Majumdar S, Housseau F, Pardoll DM, Elisseeff JH, Divergent immune responses to synthetic and biological scaffolds, Biomaterials. 192 (2019) 405–415. 10.1016/J.BIOMATERIALS.2018.11.002. [PubMed: 30500722]

[30]. Hu S, Kuwabara R, Navarro Chica CE, Smink AM, Koster T, Medina JD, de Haan BJ, Beukema M, Lakey JRT, García AJ, de Vos P, Toll-like receptor 2-modulating pectin-polymers in alginate-based microcapsules attenuate immune responses and support islet-xenograft survival, Biomaterials. 266 (2021) 120460. 10.1016/J.BIOMATERIALS.2020.120460.

[31]. Rogers TH, Babensee JE, Altered adherent leukocyte profile on biomaterials in Toll-like receptor 4 deficient mice, Biomaterials. 31 (2010) 594–601. 10.1016/J.BIOMATERIALS.2009.09.077. [PubMed: 19818491]

[32]. Chu C, Zhao X, Rung S, Xiao W, Liu L, Qu Y, Man Y, Application of biomaterials in periodontal tissue repair and reconstruction in the presence of inflammation under periodontitis through the foreign body response: Recent progress and perspectives, J Biomed Mater Res B Appl Biomater. 110 (2022) 7–17. 10.1002/JBM.B.34891. [PubMed: 34142745]

[33]. Wooley PH, Morren R, Andary J, Sud S, Yang SY, Mayton L, Markel D, Sieving A, Nasser S, Inflammatory responses to orthopaedic biomaterials in the murine air pouch, Biomaterials. 23 (2002) 517–526. 10.1016/S0142-9612(01)00134-X. [PubMed: 11761173]

[34]. Abaricia JO, Farzad N, Heath TJ, Simmons J, Morandini L, Olivares-Navarrete R, Control of innate immune response by biomaterial surface topography, energy, and stiffness, Acta Biomater. 133 (2021) 58–73. 10.1016/J.ACTBIO.2021.04.021. [PubMed: 33882355]

[35]. Abaricia JO, Shah AH, Chaubal M, Hotchkiss KM, Olivares-Navarrete R, Wnt signaling modulates macrophage polarization and is regulated by biomaterial surface properties, Biomaterials. 243 (2020). 10.1016/j.biomaterials.2020.119920.

[36]. Hotchkiss KM, Ayad NB, Hyzy SL, Boyan BD, Olivares-Navarrete R, Dental implant surface chemistry and energy alter macrophage activation in vitro, Clin Oral Implants Res. 28 (2017) 414–423. 10.1111/CLR.12814. [PubMed: 27006244]

[37]. Hotchkiss KM, Reddy GB, Hyzy SL, Schwartz Z, Boyan BD, Olivares-Navarrete R, Titanium surface characteristics, including topography and wettability, alter macrophage activation, Acta Biomater. 31 (2016) 425–434. 10.1016/J.ACTBIO.2015.12.003. [PubMed: 26675126]

[38]. Avery D, Morandini L, Sheakley LS, Shah AH, Bui L, Abaricia JO, Olivares-Navarrete R, Canonical Wnt signaling enhances pro-inflammatory response to titanium by macrophages, Biomaterials. 289 (2022) 121797. 10.1016/J.BIOMATERIALS.2022.121797.

[39]. Hotchkiss KM, Clark NM, Olivares-Navarrete R, Macrophage response to hydrophilic biomaterials regulates MSC recruitment and T-helper cell populations, Biomaterials. 182 (2018) 202–215. 10.1016/J.BIOMATERIALS.2018.08.029. [PubMed: 30138783]

[40]. Abaricia JO, Shah AH, Ruzga MN, Olivares-Navarrete R, Surface characteristics on commercial dental implants differentially activate macrophages in vitro and in vivo, Clin Oral Implants Res. 32 (2021) 487–497. 10.1111/CLR.13717. [PubMed: 33502059]

[41]. Trindade R, Albrektsson T, Galli S, Prgomet Z, Tengvall P, Wennerberg A, Bone Immune Response to Materials, Part I: Titanium, PEEK and Copper in Comparison to Sham at 10 Days in Rabbit Tibia, Journal of Clinical Medicine 2018, Vol. 7, Page 526. 7 (2018) 526. 10.3390/JCM7120526.

[42]. Trindade R, Albrektsson T, Galli S, Prgomet Z, Tengvall P, Wennerberg A, Bone Immune Response to Materials, Part II: Copper and Polyetheretherketone (PEEK) Compared to Titanium at 10 and 28 Days in Rabbit Tibia, Journal of Clinical Medicine 2019, Vol. 8, Page 814. 8 (2019) 814. 10.3390/JCM8060814.

[43]. Blum C, Berat Taskin M, Shan J, Schilling T, Schlegelmilch K, Teßmar J, Groll J, Blum C, Taskin MB, Shan J, Schilling T, Schlegelmilch K, Teßmar J, Groll J, Appreciating the First Line of the Human Innate Immune Defense: A Strategy to Model and Alleviate the Neutrophil Elastase-Mediated Attack toward Bioactivated Biomaterials, (2021). 10.1002/smll.202007551.

[44]. Abaricia JO, Shah AH, Musselman RM, Olivares-Navarrete R, Hydrophilic titanium surfaces reduce neutrophil inflammatory response and NETosis, Biomater Sci. 8 (2020) 2289–2299. 10.1039/C9BM01474H. [PubMed: 32163073]

[45]. Nolan E, Malanchi I, Connecting the dots: Neutrophils at the interface of tissue regeneration and cancer, Semin Immunol. 57 (2021). 10.1016/J.SMIM.2022.101598.

[46]. Abaricia JO, Shah AH, Olivares-Navarrete R, Substrate stiffness induces neutrophil extracellular trap (NET) formation through focal adhesion kinase activation, Biomaterials. 271 (2021) 120715. 10.1016/J.BIOMATERIALS.2021.120715.

[47]. Stephen J, Scales HE, Benson RA, Erben D, Garside P, Brewer JM, Neutrophil swarming and extracellular trap formation play a significant role in Alum adjuvant activity, Npj Vaccines 2017 2:1. 2 (2017) 1–9. 10.1038/s41541-016-0001-5.

[48]. Chang S, Popowich Y, Greco RS, Haimovich B, Neutrophil survival on biomaterials is determined by surface topography, J Vasc Surg. 37 (2003) 1082–1090. 10.1067/MVA.2003.160. [PubMed: 12756358]

[49]. Ruterbusch M, Pruner KB, Shehata L, Pepper M, In Vivo CD4+ T Cell Differentiation and Function: Revisiting the Th1/Th2 Paradigm, 10.1146/Annurev-Immunol-103019-085803. 38 (2020) 705–725. 10.1146/ANNUREV-IMMUNOL-103019-085803.

[50]. Adusei KM, Ngo TB, Sadtler K, T lymphocytes as critical mediators in tissue regeneration, fibrosis, and the foreign body response, Acta Biomater. 133 (2021) 17–33. 10.1016/J.ACTBIO.2021.04.023. [PubMed: 33905946]

[51]. Szabo SJ, Sullivan BM, Peng SL, Glimcher LH, Molecular mechanisms regulating Th1 immune responses, Annu Rev Immunol. 21 (2003) 713–758. 10.1146/ANNUREV.IMMUNOL.21.120601.140942. [PubMed: 12500979]

[52]. Kopf M, le Gros G, Bachmann M, Lamers MC, Bluethmann H, Köhler G, Disruption of the murine IL-4 gene blocks Th2 cytokine responses, Nature. 362 (1993) 245–248. 10.1038/362245A0. [PubMed: 8384701]

[53]. Coffman RL, Seymour BWP, Hudak S, Jackson J, Rennick D, Antibody to interleukin-5 inhibits helminth-induced eosinophilia in mice, Science. 245 (1989) 308–310. 10.1126/SCIENCE.2787531. [PubMed: 2787531]

[54]. Gordon S, Alternative activation of macrophages, Nat Rev Immunol. 3 (2003) 23–35. 10.1038/NRI978. [PubMed: 12511873]

[55]. Ouyang W, Kolls JK, Zheng Y, The biological functions of T helper 17 cell effector cytokines in inflammation, Immunity. 28 (2008) 454–467. 10.1016/J.IMMUNI.2008.03.004. [PubMed: 18400188]

[56]. Korn T, Bettelli E, Oukka M, Kuchroo VK, IL-17 and Th17 Cells, Annu Rev Immunol. 27 (2009) 485–517. 10.1146/ANNUREV.IMMUNOL.021908.132710. [PubMed: 19132915]

[57]. Iwakura Y, Ishigame H, Saijo S, Nakae S, Functional specialization of interleukin-17 family members, Immunity. 34 (2011) 149–162. 10.1016/J.IMMUNI.2011.02.012. [PubMed: 21349428]

[58]. Bilate AM, Lafaille JJ, Induced CD4+Foxp3+ regulatory T cells in immune tolerance, Annu Rev Immunol. 30 (2012) 733–758. 10.1146/ANNUREV-IMMUNOL-020711-075043. [PubMed: 22224762]

[59]. Gretzer C, Emanuelsson L, Liljensten E, Thomsen P, The inflammatory cell influx and cytokines changes during transition from acute inflammation to fibrous repair around implanted materials, J Biomater Sci Polym Ed. 17 (2006) 669–687. 10.1163/156856206777346340. [PubMed: 16892728]

[60]. Yang W, Tao Y, Wu Y, Zhao X, Ye W, Zhao D, Fu L, Tian C, Yang J, He F, Tang L, Neutrophils promote the development of reparative macrophages mediated by ROS to orchestrate liver repair, Nature Communications 2019 10:1. 10 (2019) 1–14. 10.1038/s41467-019-09046-8.

[61]. Kolaczkowska E, Kubes P, Neutrophil recruitment and function in health and inflammation, Nature Reviews Immunology 2013 13:3. 13 (2013) 159–175. 10.1038/nri3399.

[62]. Ng LG, Qin JS, Roediger B, Wang Y, Jain R, Cavanagh LL, Smith AL, Jones CA, de Veer M, Grimbaldeston MA, Meeusen EN, Weninger W, Visualizing the neutrophil response to sterile tissue injury in mouse dermis reveals a three-phase cascade of events, J Invest Dermatol. 131 (2011) 2058–2068. 10.1038/JID.2011.179. [PubMed: 21697893]

[63]. Dallegri F, Ottonello L, Tissue injury in neutrophilic inflammation, Inflamm Res. 46 (1997) 382–391. 10.1007/S000110050208. [PubMed: 9372309]

[64]. Kruger P, Saffarzadeh M, Weber ANR, Rieber N, Radsak M, von Bernuth H, Benarafa C, Roos D, Skokowa J, Hartl D, Neutrophils: Between host defence, immune modulation, and tissue injury, PLoS Pathog. 11 (2015) 1–22. 10.1371/JOURNAL.PPAT.1004651.

[65]. Jhunjhunwala S, Neutrophils at the Biological-Material Interface, ACS Biomater Sci Eng. 4 (2018) 1128–1136. 10.1021/ACSBIOMATERIALS.6B00743/ASSET/IMAGES/LARGE/AB-2016-00743J_0003.JPEG. [PubMed: 33418651]

[66]. Zhou Z, Zhang S, Ding S, Abudupataer M, Zhang Z, Zhu X, Zhang W, Zou Y, Yang X, Ge J, Hong T, Excessive neutrophil extracellular trap formation aggravates acute myocardial infarction injury in apolipoprotein e deficiency mice via the ROS-dependent pathway, Oxid Med Cell Longev. 2019 (2019). 10.1155/2019/1209307.

[67]. Narasaraju T, Yang E, Samy RP, Ng HH, Poh WP, Liew AA, Phoon MC, van Rooijen N, Chow VT, Excessive Neutrophils and Neutrophil Extracellular Traps Contribute to Acute Lung Injury of Influenza Pneumonitis, Am J Pathol. 179 (2011) 199–210. 10.1016/J.AJPATH.2011.03.013. [PubMed: 21703402]

[68]. Deshmane SL, Kremlev S, Amini S, Sawaya BE, Monocyte chemoattractant protein-1 (MCP-1): an overview, J Interferon Cytokine Res. 29 (2009) 313–325. 10.1089/JIR.2008.0027. [PubMed: 19441883]

[69]. Camarero-Espinosa S, Carlos-Oliveira M, Liu H, Mano JF, Bouvy N, Moroni L, 3D Printed Dual-Porosity Scaffolds: The Combined Effect of Stiffness and Porosity in the Modulation of Macrophage Polarization, (2021). 10.1002/adhm.202101415.

[70]. Sussman EM, Halpin MC, Muster J, Moon RT, Ratner BD, Porous implants modulate healing and induce shifts in local macrophage polarization in the foreign body reaction, Ann Biomed Eng. 42 (2014) 1508–1516. 10.1007/S10439-013-0933-0/FIGURES/4. [PubMed: 24248559]

[71]. Warnatsch A, Ioannou M, Wang Q, Papayannopoulos V, Inflammation. Neutrophil extracellular traps license macrophages for cytokine production in atherosclerosis, Science. 349 (2015) 316–320. 10.1126/SCIENCE.AAA8064. [PubMed: 26185250]

[72]. Grattendick K, Stuart R, Roberts E, Lincoln J, Lefkowitz SS, Bollen A, Moguilevsky N, Friedman H, Lefkowitz DL, Alveolar macrophage activation by myeloperoxidase: a model for exacerbation of lung inflammation, Am J Respir Cell Mol Biol. 26 (2002) 716–722. 10.1165/AJRCMB.26.6.4723. [PubMed: 12034571]

[73]. Krotova K, Khodayari N, Oshins R, Aslanidi G, Brantly ML, Neutrophil elastase promotes macrophage cell adhesion and cytokine production through the integrin-Src kinases pathway, Sci Rep. 10 (2020). 10.1038/S41598-020-72667-3.

[74]. Ellen RP, Microbial colonization of the peri-implant environment and its relevance to long-term success of osseointegrated implants., Int J Prosthodont. 11 (n.d.) 433–41. http://www.ncbi.nlm.nih.gov/pubmed/9922735 (accessed February 19, 2023).

[75]. Norowski PA, Bumgardner JD, Biomaterial and antibiotic strategies for peri-implantitis, J Biomed Mater Res B Appl Biomater. 88 (2009) 530–543. 10.1002/jbm.b.31152. [PubMed: 18698626]

[76]. Stoikes NFN, Scott JR, Badhwar A, Deeken CR, Voeller GR, Characterization of host response, resorption, and strength properties, and performance in the presence of bacteria for fully absorbable biomaterials for soft tissue repair, Hernia. 21 (2017) 771–782. 10.1007/S10029-017-1638-3/FIGURES/9. [PubMed: 28815398]

[77]. Rohner NA, Learn GD, Wiggins MJ, Woofter RT, von Recum HA, Characterization of Inflammatory and Fibrotic Encapsulation Responses of Implanted Materials with Bacterial Infection, ACS Biomater Sci Eng. 7 (2021) 4474–4482. 10.1021/ACSBIOMATERIALS.1C00505/ASSET/IMAGES/LARGE/AB1C00505_0007.JPEG. [PubMed: 34464101]

[78]. Akira S, Hemmi H, Recognition of pathogen-associated molecular patterns by TLR family, Immunol Lett. 85 (2003) 85–95. 10.1016/S0165-2478(02)00228-6. [PubMed: 12527213]

[79]. Schwarz F, Alcoforado G, Guerrero A, Jönsson D, Klinge B, Lang N, Mattheos N, Mertens B, Pitta J, Ramanauskaite A, Sayardoust S, Sanz-Martin I, Stavropoulos A, Heitz-Mayfield L, Peri-implantitis: Summary and consensus statements of group 3. The 6th EAO Consensus Conference 2021, Clin Oral Implants Res. 32 Suppl 21 (2021) 245–253. 10.1111/CLR.13827. [PubMed: 34642987]

[80]. Berglundh T, Armitage G, Araujo MG, Avila-Ortiz G, Blanco J, Camargo PM, Chen S, Cochran D, Derks J, Figuero E, Hämmerle CHF, Heitz-Mayfield LJA, Huynh-Ba G, Iacono V, Koo KT, Lambert F, McCauley L, Quirynen M, Renvert S, Salvi GE, Schwarz F, Tarnow D, Tomasi C, Wang HL, Zitzmann N, Peri-implant diseases and conditions: Consensus report of workgroup 4 of the 2017 World Workshop on the Classification of Periodontal and Peri-Implant Diseases and Conditions, J Clin Periodontol. 45 Suppl 20 (2018) S286–S291. 10.1111/JCPE.12957. [PubMed: 29926491]

[81]. Daubert DM, Weinstein BF, Biofilm as a risk factor in implant treatment, Periodontol 2000. 81 (2019) 29–40. 10.1111/PRD.12280. [PubMed: 31407437]

[82]. Revell PA, The combined role of wear particles, macrophages and lymphocytes in the loosening of total joint prostheses, J R Soc Interface. 5 (2008) 1263–1278. 10.1098/RSIF.2008.0142. [PubMed: 18647740]

[83]. Horowitz SM, Purdon MA, Calcified Tissue In~ern'afional Orthopedic Surgical Forum Mechanisms of Cellular Recruitment in Aseptic Loosening of Prosthetic Joint Implants, Calcif Tissue Int. 57 (1995) 301–305. [PubMed: 8673868]

[84]. Pelletier MH, Cordaro N, Punjabi VM, Waites M, Lau A, Walsh WR, PEEK Versus Ti Interbody Fusion Devices: Resultant Fusion, Bone Apposition, Initial and 26-Week Biomechanics, Clin Spine Surg. 29 (2016) E208–E214. 10.1097/BSD.0B013E31826851A4. [PubMed: 22801456]

[85]. Toth JM, Wang M, Estes BT, Scifert JL, Seim HB, Turner AS, Polyetheretherketone as a biomaterial for spinal applications, Biomaterials. 27 (2006) 324–334. 10.1016/J.BIOMATERIALS.2005.07.011. [PubMed: 16115677]

[86]. Krzyszczyk P, Schloss R, Palmer A, Berthiaume F, The role of macrophages in acute and chronic wound healing and interventions to promote pro-wound healing phenotypes, Front Physiol. 9 (2018). 10.3389/fphys.2018.00419.

[87]. Ono T, Takayanagi H, Osteoimmunology in Bone Fracture Healing, Curr Osteoporos Rep. 15 (2017) 367–375. 10.1007/S11914-017-0381-0/FIGURES/1. [PubMed: 28647888]

[88]. Albrektsson T, Tengvall P, Amengual L, Coli P, Kotsakis GA, Cochran D, Osteoimmune regulation underlies oral implant osseointegration and its perturbation, Front Immunol. 13 (2023). 10.3389/FIMMU.2022.1056914.

[89]. Gao A, Liao Q, Xie L, Wang G, Zhang W, Wu Y, Li P, Guan M, Pan H, Tong L, Chu PK, Wang H, Tuning the surface immunomodulatory functions of polyetheretherketone for enhanced osseointegration, Biomaterials. 230 (2020). 10.1016/J.BIOMATERIALS.2019.119642.

[90]. Walsh WR, Bertollo N, Christou C, Schaffner D, Mobbs RJ, Plasma-sprayed titanium coating to polyetheretherketone improves the bone-implant interface, Spine J. 15 (2015) 1041–1049. 10.1016/J.SPINEE.2014.12.018. [PubMed: 25543010]

[91]. Torstrick FB, Lin ASP, Potter D, Safranski DL, Sulchek TA, Gall K, Guldberg RE, Porous PEEK improves the bone-implant interface compared to plasma-sprayed titanium coating on PEEK, Biomaterials. 185 (2018) 106–116. 10.1016/J.BIOMATERIALS.2018.09.009. [PubMed: 30236838]

[92]. Poulsson AHC, Eglin D, Zeiter S, Camenisch K, Sprecher C, Agarwal Y, Nehrbass D, Wilson J, Richards RG, Osseointegration of machined, injection moulded and oxygen plasma modified PEEK implants in a sheep model, Biomaterials. 35 (2014) 3717–3728. 10.1016/J.BIOMATERIALS.2013.12.056. [PubMed: 24485795]

[93]. Brodbeck WG, Nakayama Y, Matsuda T, Colton E, Ziats NP, Anderson JM, Biomaterial surface chemistry dictates adherent monocyte/macrophage cytokine expression in vitro, Cytokine. 18 (2002) 311–319. 10.1006/cyto.2002.1048. [PubMed: 12160519]

[94]. Zhou Y, Zhang H, Yao Y, Zhang X, Guan Y, Zheng F, CD4+ T cell activation and inflammation in NASH-related fibrosis, Front Immunol. 13 (2022). 10.3389/FIMMU.2022.967410.

[95]. Ritzmann F, Lunding LP, Bals R, Wegmann M, Beisswenger C, IL-17 Cytokines and Chronic Lung Diseases, Cells. 11 (2022). 10.3390/CELLS11142132.

[96]. Brodbeck WG, MacEwan M, Colton E, Meyerson H, Anderson JM, Lymphocytes and the foreign body response: lymphocyte enhancement of macrophage adhesion and fusion, J Biomed Mater Res A. 74 (2005) 222–229. 10.1002/JBM.A.30313. [PubMed: 15948198]

[97]. Guo F, Yuan C, Huang H, Deng X, Bian Z, Wang D, Dou K, Mei L, Zhou Q, Regulation of T Cell Responses by Nano-Hydroxyapatite to Mediate the Osteogenesis, Front Bioeng Biotechnol. 10 (2022). 10.3389/FBIOE.2022.884291.

[98]. Yokoyama M, Nakahashi T, Nishimura T, Maeda M, Inoue S, Kataoka K, Sakurai Y, Adhesion behavior of rat lymphocytes to poly(ether)-poly(amino acid) block and graft copolymers, J Biomed Mater Res. 20 (1986) 867–878. 10.1002/JBM.820200702. [PubMed: 3760003]

[99]. Wolfram D, Rabensteiner E, Grundtman C, Böck G, Mayerl C, Parson W, Almanzar G, Hasenöhrl C, Piza-Katzer H, Wick G, T regulatory cells and TH17 cells in peri-silicone implant capsular fibrosis, Plast Reconstr Surg. 129 (2012). 10.1097/PRS.0B013E31823AEACF.

[100]. Chung L, Maestas DR, Lebid A, Mageau A, Rosson GD, Wu X, Wolf MT, Tam AJ, Vanderzee I, Wang X, Andorko JI, Zhang H, Narain R, Sadtler K, Fan H, Čiháková D, le Saux CJ, Housseau F, Pardoll DM, Elisseeff JH, Interleukin 17 and senescent cells regulate the foreign body response to synthetic material implants in mice and humans, Sci Transl Med. 12 (2020). 10.1126/SCITRANSLMED.AAX3799.

[101]. Sadtler K, Estrellas K, Allen BW, Wolf MT, Fan H, Tam AJ, Patel CH, Luber BS, Wang H, Wagner KR, Powell JD, Housseau F, Pardoll DM, Elisseeff JH, Developing a pro-regenerative biomaterial scaffold microenvironment requires T helper 2 cells, Science. 352 (2016) 366–370. 10.1126/SCIENCE.AAD9272. [PubMed: 27081073]

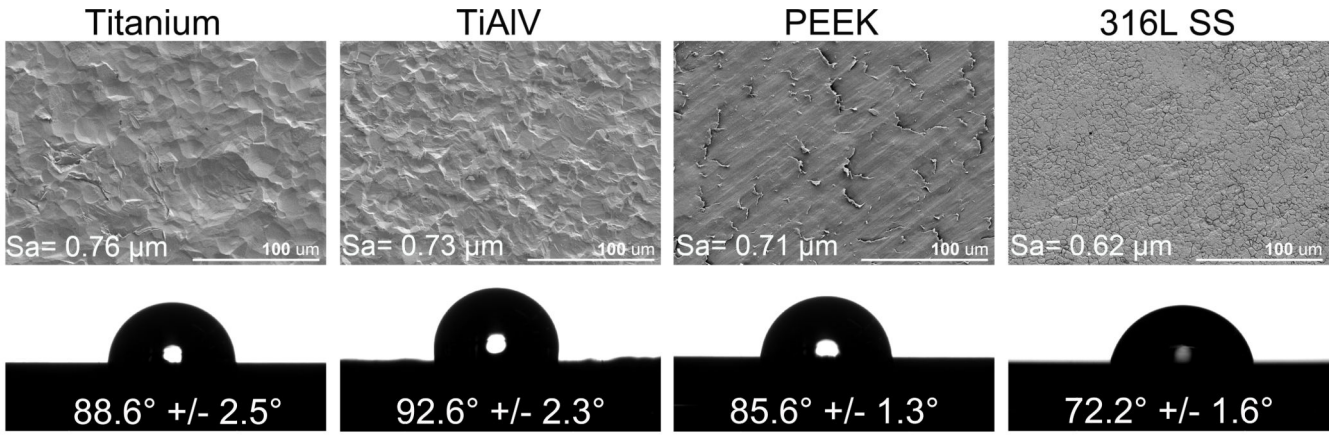

	Titanium	TiAlV	SS	PEEK
Ti	18%	14%	0%	0%
O	43%	41%	48%	17.5%
C	38%	28%	18%	82.5%
N	1%	0%	0%	0%
Al	0%	13%	0%	0%
V	0%	3%	0%	0%
Cr	0%	0%	4%	0%
Fe	0%	0%	28%	0%
Mo	0%	0%	1%	0%

Figure 1:

Characterization of Titanium, TiAlV, PEEK, and SS samples. Qualitative assessment of surface topography through scanning electron microscopy at 500X, and quantitative surface roughness (Sa) measurement by Laser Scanning Confocal Microscopy. (B) Contact angle measurements. (C) Elemental analysis of the outmost layer by XPS.

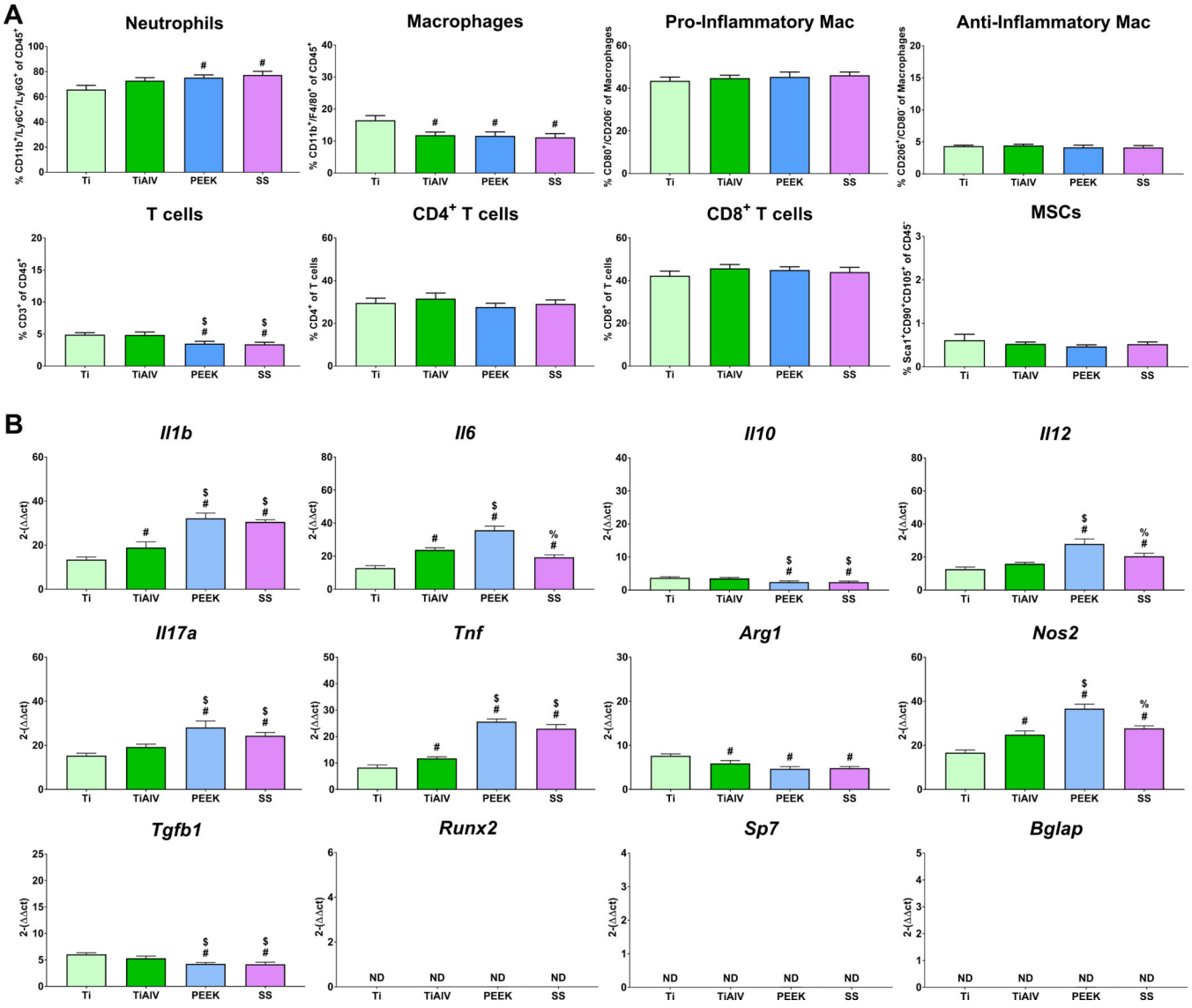

Figure 2:

Biomaterial composition alter immune cell recruitment, and inflammatory gene expression 1 day post-implantation. (A) Immunophenotyping of peri-implant bone marrow and (B) gene expression of inflammatory and osteogenic genes in C57BL/6 mice. $p<0.05$: # vs. Ti, $ vs. TiAlV, % vs. PEEK.

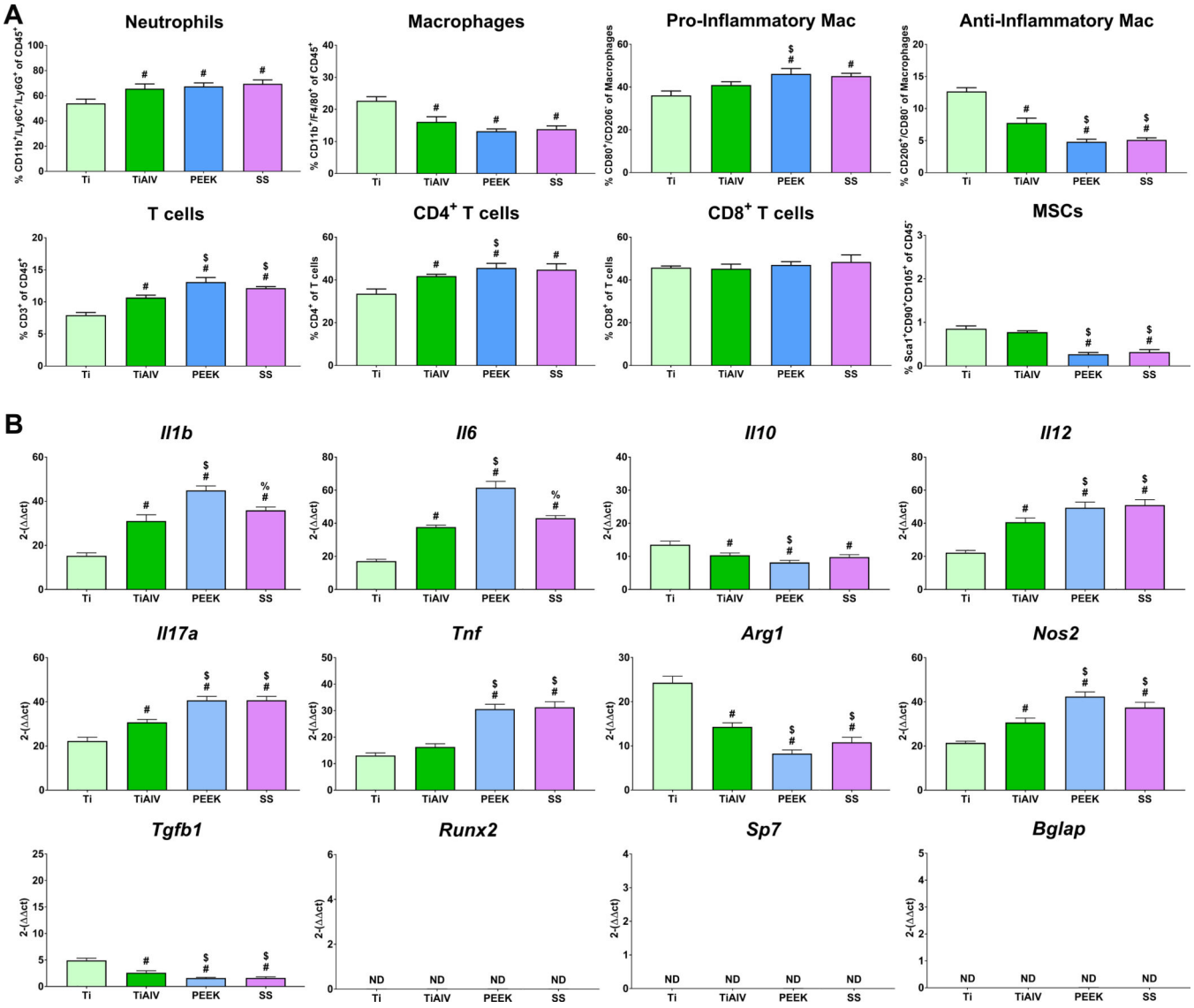

Figure 3:

Biomaterial composition alter immune cell recruitment, and inflammatory gene expression 3 day post-implantation. ((A) Immunophenotyping of peri-implant bone marrow and (B) gene expression of inflammatory and osteogenic genes in C57BL/6 mice. $p<0.05$: # vs. Ti, $ vs. TiAlV, % vs. PEEK.

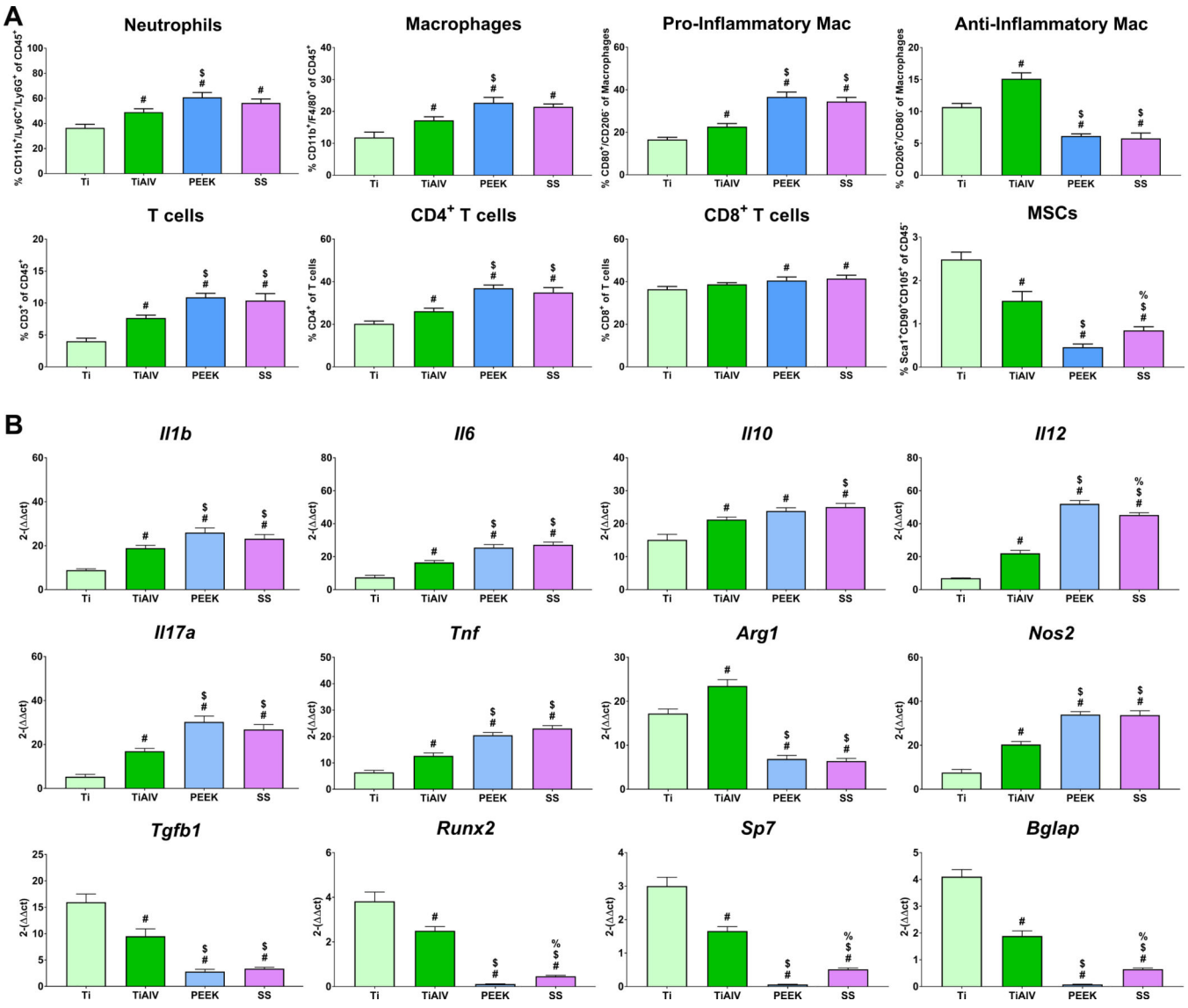

Figure 4:

Biomaterial composition alter immune cell recruitment, and inflammatory gene expression 7 day post-implantation. (A) Immunophenotyping of peri-implant bone marrow and (B) gene expression of inflammatory and osteogenic genes in C57BL/6 mice. $p<0.05$: # vs. Ti, $ vs. TiAlV, % vs. PEEK.

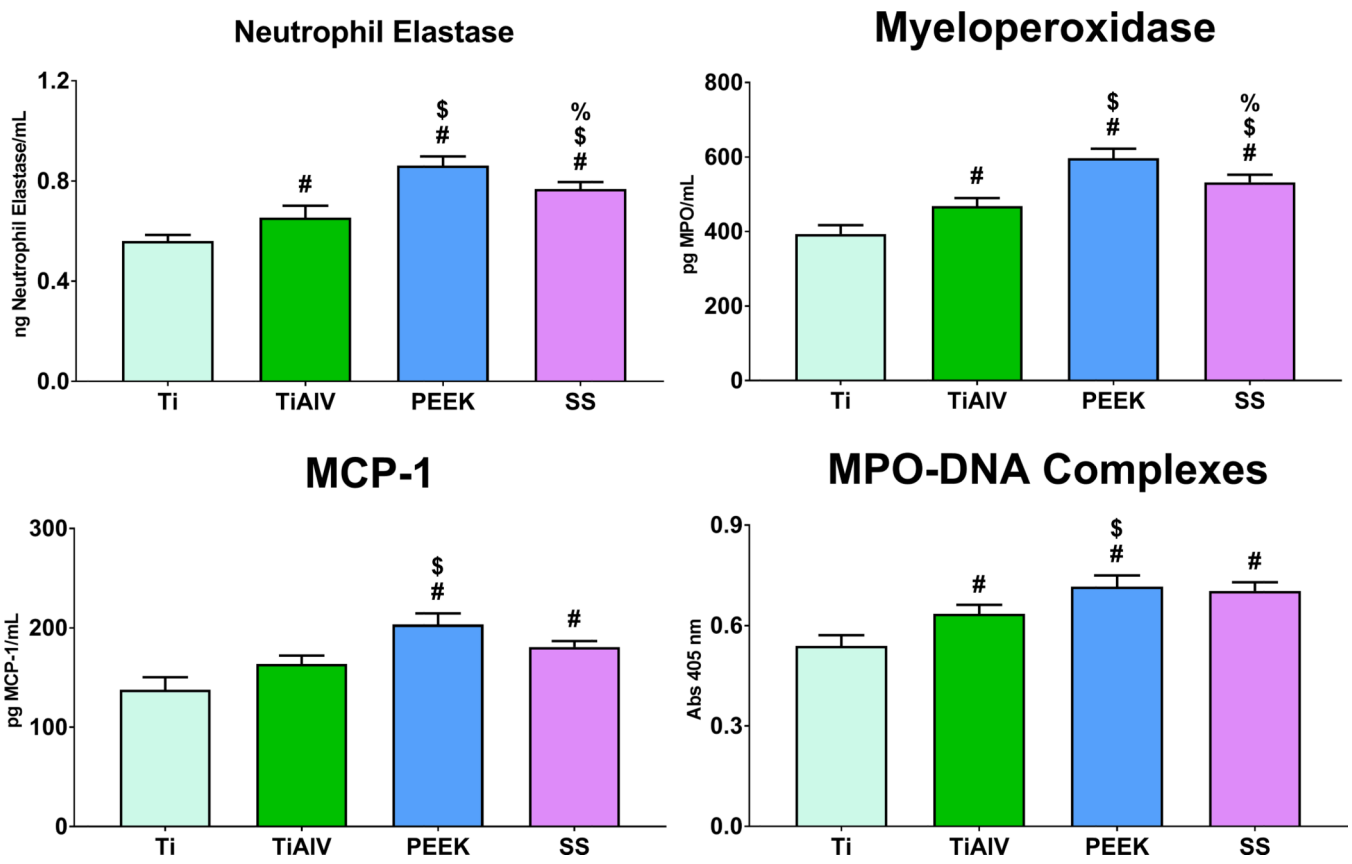

Figure 5:

PEEK and 316L stainless steel Increase MPO, NE, and NET formation. Analysis of NE, MPO, MCP-1 and MPO-DNA complexes in conditioned media of neutrophils cultured on either Ti, TiAlV, PEEK, or SS surfaces for 4 hours. $p<0.05$: # vs. Ti, $ vs. TiAlV, % vs. PEEK.

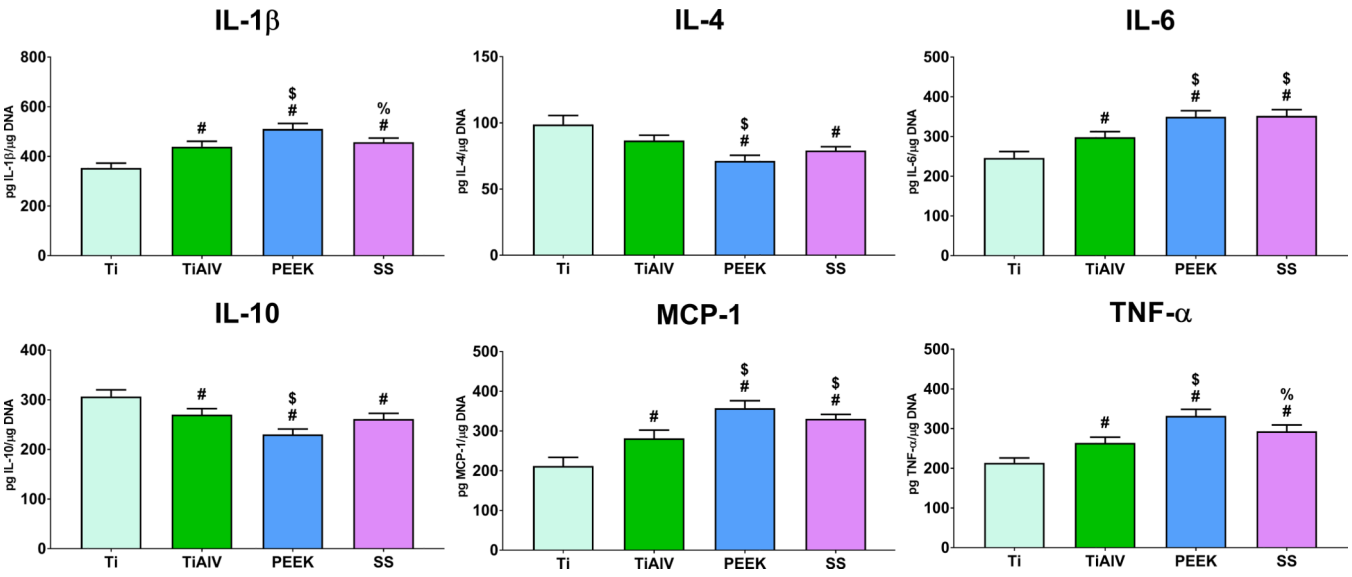

Figure 6:

Macrophages cultured on PEEK and SS produce higher pro-inflammatory microenvironment. Pro- and anti-inflammatory cytokine analysis in conditioned media of macrophages cultured on either Ti, TiAlV, PEEK, or SS surfaces for 24 hours. $p<0.05$: # vs. Ti, $ vs. TiAlV, % vs. PEEK.

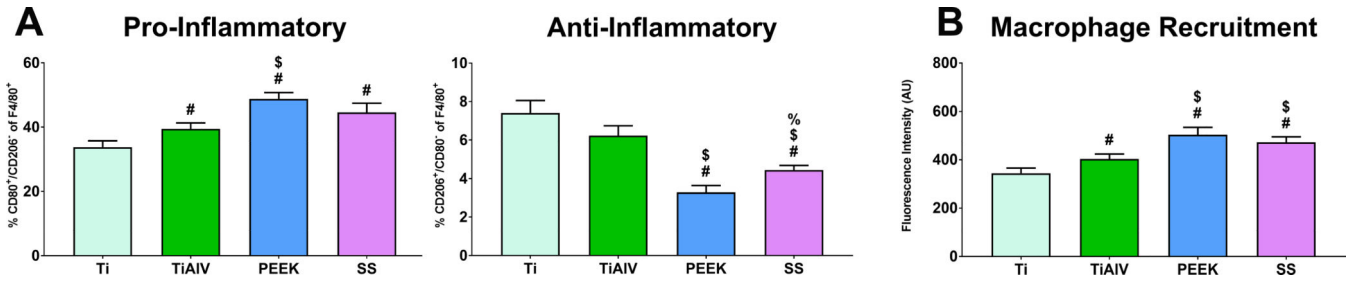

Figure 7:

Neutrophil response to PEEK and SS increased pro-inflammatory macrophage activation and macrophage recruitment in vitro. (A) Flow cytometry analysis of macrophage phenotype after co-culture with neutrophils on either Ti, TiAlV, PEEK, or SS surfaces for 24 hours. $p<0.05$: # vs. Ti, $ vs. TiAlV, % vs. PEEK.

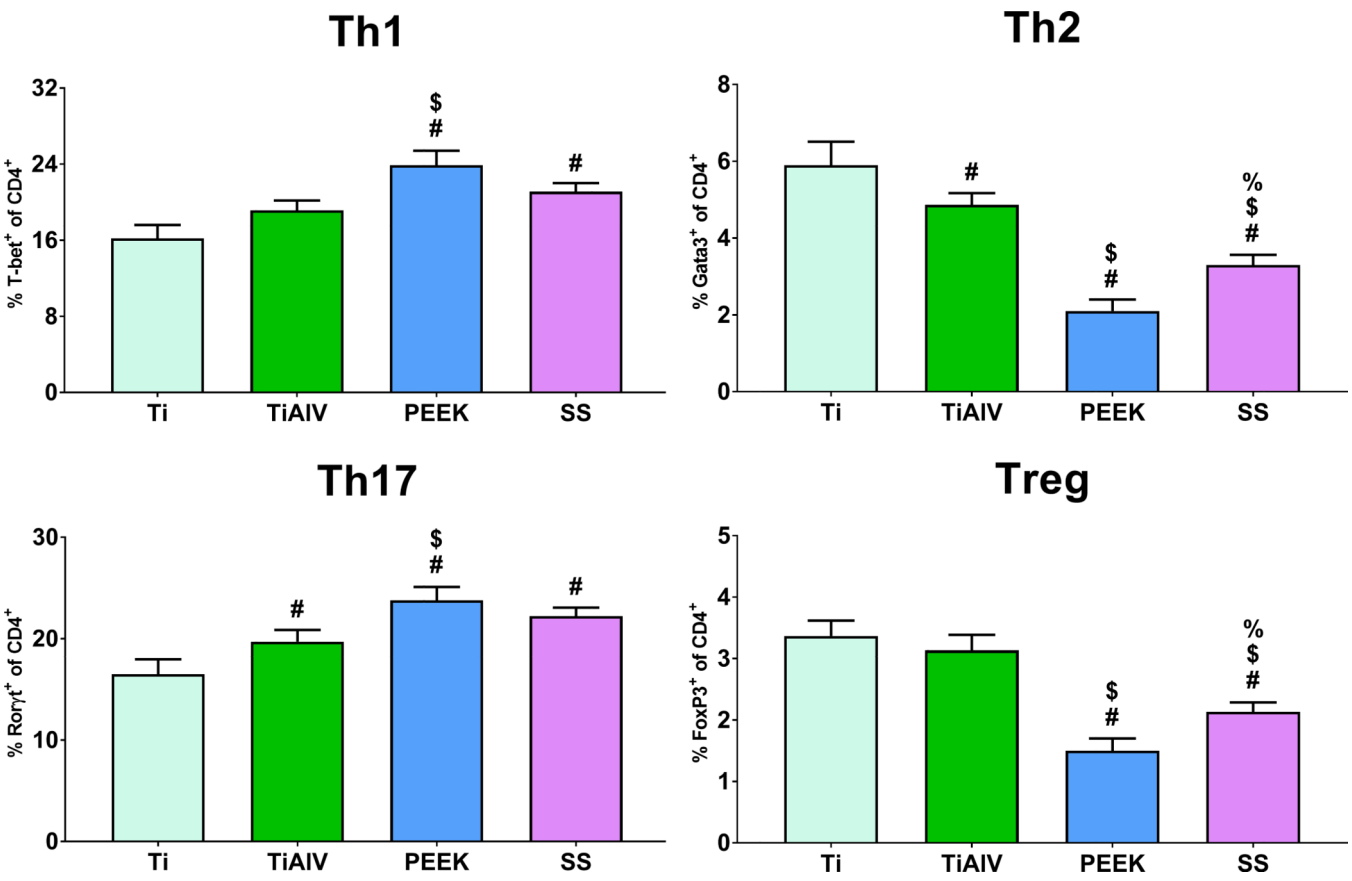

Figure 8:

Macrophage response to PEEK and SS increased $CD4^+$ T cell polarization towards Th1 and Th17 subsets *in vitro*. Flow cytometry analysis of $CD4^+$ T cells co-cultured with macrophages on either Ti, TiAlV, PEEK, or SS surfaces for 48 hours. $p<0.05$: # vs. Ti, $ vs. TiAlV, % vs. PEEK.

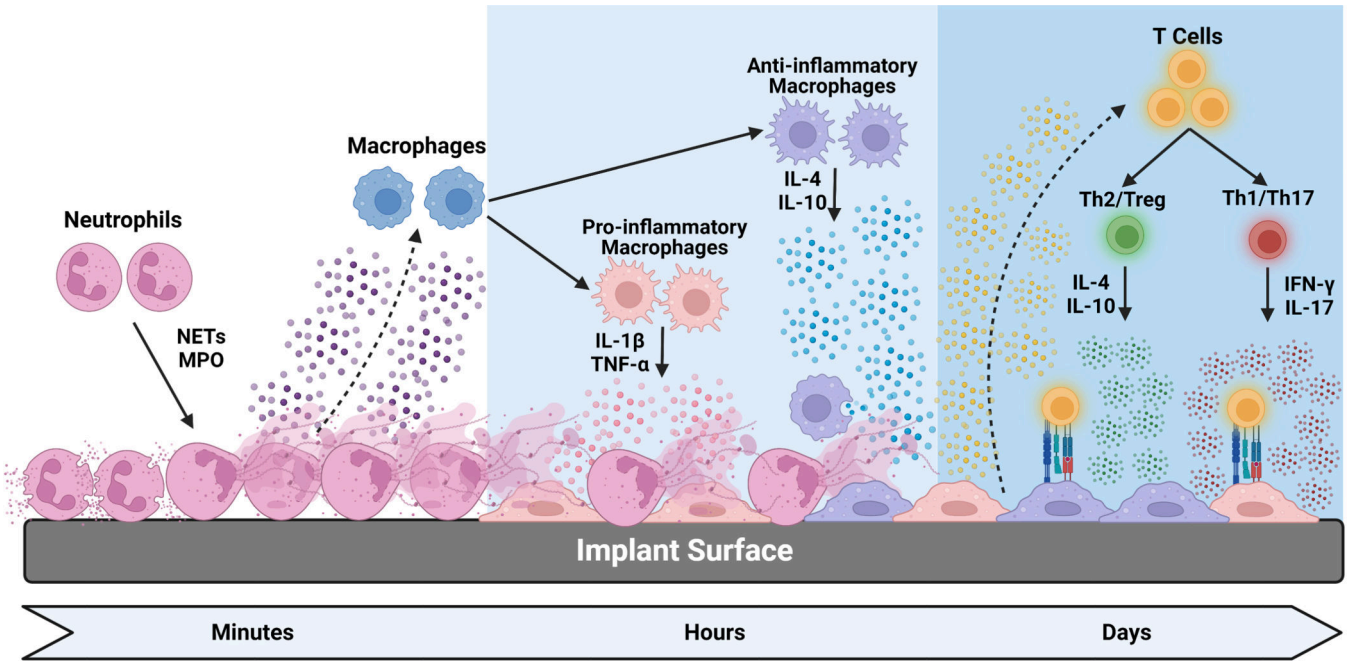

Figure 9.

Diagram summarizing the immune cell-biomaterial interactions and the direct and indirect immune cell interactions from our experiments.